CD146 is a potential immunotarget for neuroblastoma

AUTHOR(S):

Obu, Satoshi; Umeda, Katsutsugu; Ueno, Hiroo; Sonoda, Mari; Tasaka, Keiji; Ogata, Hideto; Kouzuki, Kagehiro; ... Uemoto, Shinji; Heike, Toshio; Takita, Junko

CITATION:

Obu, Satoshi ...[et al]. CD146 is a potential immunotarget for neuroblastoma. Cancer Science 2021, 112(11): 4617-4626

ISSUE DATE:

2021-08-31

URL:

http://hdl.handle.net/2433/277489

Received: 27 May 2021 | Revised: 13 August 2021 | Accepted: 26 August 2021

DOI: 10.1111/cas.15124

ORIGINAL ARTICLE

Cancer Science WILEY

CD146 is a potential immunotarget for neuroblastoma

Satoshi Obu[1] | Katsutsugu Umeda[1] | Hiroo Ueno[1] | Mari Sonoda[2] | Keiji Tasaka[1] | Hideto Ogata[1] | Kagehiro Kouzuki[1] | Seishiro Nodomi[1] | Satoshi Saida[1] | Itaru Kato[1] | Hidefumi Hiramatsu[1] | Tatsuya Okamoto[2] | Eri Ogawa[2] | Hideaki Okajima[2,3] | Ken Morita[4] | Yasuhiko Kamikubo[4] | Koji Kawaguchi[5] | Kenichiro Watanabe[5] | Hideto Iwafuchi[6] | Shigeki Yagyu[7] | Tomoko Iehara[7] | Hajime Hosoi[7] | Tatsutoshi Nakahata[8] | Souichi Adachi[4] | Shinji Uemoto[2] | Toshio Heike[1] | Junko Takita[1]

[1]Department of Pediatrics, Graduate School of Medicine, Kyoto University, Kyoto, Japan

[2]Department of Pediatric Surgery, Graduate School of Medicine, Kyoto University, Kyoto, Japan

[3]Department of Pediatric Surgery, Kanazawa Medical University, Ishikawa, Japan

[4]Department of Human Health Science, Graduate School of Medicine, Kyoto University, Kyoto, Japan

[5]Department of Hematology and Oncology, Shizuoka Children's Hospital, Shizuoka, Japan

[6]Department of Pathology, Shizuoka Children's Hospital, Shizuoka, Japan

[7]Department of Pediatrics, Graduate School of Medical Science, Kyoto Prefectural University of Medicine, Kyoto, Japan

[8]Drug Discovery Technology Development Office, Center for iPS Cell Research and Application, Kyoto University, Kyoto, Japan

Correspondence
Katsutsugu Umeda, MD, PhD, Department of Pediatrics, Graduate School of Medicine, Kyoto University, 54 Kawahara-cho, Shogoin, Sakyo-ku, Kyoto 606-8507, Japan.
Email: umeume@kuhp.kyoto-u.ac.jp

Funding information
Japan Agency for Medical Research and Development, Grant/Award Number: 19ck0106468h0001

Abstract

Neuroblastoma, the most common extracranial solid tumor of childhood, is thought to arise from neural crest-derived immature cells. The prognosis of patients with high-risk or recurrent/refractory neuroblastoma remains quite poor despite intensive multimodality therapy; therefore, novel therapeutic interventions are required. We examined the expression of a cell adhesion molecule CD146 (melanoma cell adhesion molecule [MCAM]) by neuroblastoma cell lines and in clinical samples and investigated the anti-tumor effects of CD146-targeting treatment for neuroblastoma cells both in vitro and in vivo. CD146 is expressed by 4 cell lines and by most of primary tumors at any stage. Short hairpin RNA-mediated knockdown of CD146, or treatment with an anti-CD146 polyclonal antibody, effectively inhibited growth of neuroblastoma cells both in vitro and in vivo, principally due to increased apoptosis via the focal adhesion kinase and/or nuclear factor-kappa B signaling pathway. Furthermore, the anti-CD146 polyclonal antibody markedly inhibited tumor growth in immunodeficient mice inoculated with primary neuroblastoma cells. In conclusion, CD146 represents a promising therapeutic target for neuroblastoma.

KEYWORDS

antibody, apoptosis, CD146, focal adhesion kinase, neuroblastoma

Abbreviations: AAD, Amino-actinomycin D; ADCC, antibody-dependent cellular cytotoxicity; APC, allophycocyanin; CI, confidence interval; FAK, focal adhesion kinase; Luc, luciferase; MCAM, melanoma cell adhesion molecule; MFI, mean fluorescence intensity; NB, neuroblastoma; NC, neural crest; NF-κB, nuclear factor-kappa B; NOG, NOD/Shi-scid IL-2Rγ-null; OS, overall survival; PE, phycoerythrin; PFS, progression-free survival; Sh, short hairpin; TARGET, Therapeutically Applicable Research to Generate Effective Treatment.

1 | INTRODUCTION

Neuroblastoma is the most common extracranial solid tumor of childhood, accounting for ~15% of cancer-related deaths in pediatric patients under the age of 15 y.[1] The disease is highly heterogenous, with prognoses ranging from spontaneous regression without treatment to a dismal outcome. Risk-stratified treatment based on clinicopathological (ie, age at diagnosis, stage, and histology) and genetic (ie, MYCN amplification and ploidy) prognostic factors has led to a marked improvement in outcome for patients with low-risk or intermediate-risk NB. However, the prognosis for those with high-risk, recurrent, or refractory NB remains dismal, despite intensive multimodality therapy.[2,3] In addition, long-term NB survivors are at risk of developing late adverse effects such as renal impairment, endocrine disturbance, dental defects, and secondary malignancies.[4] Patients with minimal residual disease can be treated with an anti-GD2 monoclonal antibody, with significant clinical benefit.[5] However, this therapy remains unsatisfactory for patients with measurable tumors.[6] Therefore, more effective and less toxic therapies are warranted.

NB is thought to originate from NC-derived immature cells. NC is a transient population of multipotent progenitors that arises at the neural plate border in vertebrate embryos before migrating throughout the body to generate various tissues, including bones, neurons, glia, and melanocytes.[7] CD146 (melanoma cell adhesion molecule [MCAM]) is a cell adhesion molecule belonging to the immunoglobulin superfamily. The *CD146* gene is located on chromosome 11q23.3.[8] In adults, expression of CD146 is restricted to a limited number of normal tissues, including endothelium, smooth muscle, ganglion cells, Schwann cells, cerebellar cortex, and activated T lymphocytes.[9-11] By contrast, it is expressed widely in embryonic tissues, including NC and its derivatives.[12] CD146 plays an active role in a variety of process, including in cell-cell and cell-matrix interactions, cell migration, signal transduction, immune responses, and embryonic development.[10] Growing evidence has shown that CD146 promotes tumor progression and metastasis, and is a promising candidate for immunotherapy in various malignancies, including NC-derived melanoma, malignant rhabdoid tumor, and NB.[11,13-16] However, the potential of CD146 as a therapeutic target for NB remains unclear.

Here, we examined the expression of CD146 by NB cell lines and in clinical samples and investigated the anti-tumor effects of CD146-targeting treatment for NB cells both in vitro and in vivo.

2 | MATERIALS AND METHODS

2.1 | Cell lines, tumor samples, and animals

Human NB cell lines (IMR-32, SK-N-SH, RT-BM1, and SK-N-SIFA), established as reported previously,[17] were cultured in RPMI-1640 medium containing penicillin, streptomycin, L-glutamine, and 10% heat-inactivated FBS. All NB cells lines were authenticated by short tandem repeat-based DNA analysis. The Mewo human melanoma cell line was purchased from the American Type Culture Collection (Manassas, VA, USA) and cultured in DMEM containing penicillin, streptomycin, L-glutamine, and 10% FBS. HUVECs were purchased from BD Biosciences (New Jersey, USA) and cultured in Endothelial Cell Growth Medium 2 (PromoCell). The study was approved by the Ethics Committee of Kyoto University, and informed consent was obtained from a parent and/or legal guardian in accordance with the Declaration of Helsinki. Diagnosis of NB was made according to imaging, histological findings, and elevated expression of tumor markers. Histological classification and staging were performed according to previous reports.[18,19] All experiments involving mice were approved by the Institute of Laboratory Animals at the Graduate School of Medicine, Kyoto University. NOD/Shi-scid IL-2Rγ-null (NOG) mice were obtained from the Central Institute of Experimental Animals (Kawasaki, Japan) and used at 8-12 wk of age. Mice were housed in sterile enclosures under specific pathogen-free conditions and assigned randomly to groups prior to the experiments. Mice were anesthetized with isoflurane for all procedures and euthanized by CO_2 inhalation at the end of the experiment.

2.2 | Flow-cytometric analysis

Staining procedures, flow-cytometric analysis, and cell sorting were performed as reported previously.[15] The primary antibodies used for the analysis were listed in Table S1A. Primary tumors and xenografted tumors were co-stained with anti-human CD45, CD34, and CD31 antibodies to identify or exclude hematopoietic and endothelial cells, whereas the anti-TRA-1-85 antibody was used to distinguish human-derived cells from mouse-derived cells. Non-viable cells were excluded by co-staining with Cytox Blue dead-cell stain (Molecular Probes).

2.3 | Sphere-forming assay

Single cells were plated in triplicate in Methocult H4100 methylcellulose medium (StemCell Technologies) supplemented with 10 ng/ml human recombinant epidermal growth factor (Sigma-Aldrich), 10 ng/ml human recombinant basic fibroblast growth factor (Invitrogen), and B27 supplement (50×; Invitrogen). At 15 d later, spheres measuring ≥100 μm in diameter were counted under an Olympus CKX31 microscope (Olympus).

2.4 | Immunohistochemistry and immunofluorescence analysis

Fixation and staining of tissue samples were performed as previously described.[15] The primary antibodies used for the analysis are listed in Table S1B. CD146 positivity of tumor samples was semi-quantitatively evaluated using an H-score in immunohistochemistry, as described in a previous report.[20] Briefly, the samples were scored

according to the fraction of stained cells at each intensity. The staining intensity of the cell membrane was scored within a scale ranging from 0 to 3 as follows: 0, no staining; 1+, weak staining (ie, light brown membrane staining); 2+, intermediate staining; 3+ strong staining (ie, dark brown linear membrane staining). The CD146 H-score was calculated using the following formula: 1 × (percentage of 1+ cells) + 2 × (percentage of 2+ cells) + 3 × (percentage of 3+ cells) and defined as a continuous variable ranging from 0 to 300. A tumor sample with a CD146 H-score of <200 or ≥200 was defined as $CD146^{low}$ or $CD146^{high}$, respectively, according to the previous report.[20] The number of blood vessels per tumor in each group was quantified in at least 5 random areas per section. Images were taken on a KEYENCE BZ-X710 microscope.

2.5 | Analysis of deposit whole exome and transcriptome sequencing data

Copy-number changes were evaluated by using our in-house pipeline "CNACS." CNACS is a Unix-based program for sequencing-based copy-number analysis, and is available at (https://github.com/papaemmelab/toil_cnacs). For expression analysis, mapped reads were counted for each gene using our in-house GenomonExpression pipeline.

2.6 | Western blotting

Western blotting was performed as described previously.[15] The primary antibodies used for the analysis are listed in Table S1C. In some experiments, intensities of resulting bands were quantified densitometrically using the ChemiDoc™ XRS+System with Image Lab™ software (Bio-Rad).

2.7 | Transduction of NB cell lines with doxycycline-inducible short hairpin RNA

Lentivirus was produced and transduced as described previously.[21] Specific shRNAs targeting human CD146 and non-targeting control shRNA (for Luc) were designed and subcloned into the pENTR4-H1tetOx1, CS-RfA-ETV, and CS-RfA-ETR vectors (RIKEN BRC), as previously reported.[21] The sequences used were as follows: CD146-shRNA1, 5′-AGTTGAAGTTAAGTCAGAT-3′; CD146-shRNA2, 5′-ACACATTATGGCTGTAAAT-3′; Luc-shRNA, 5′-CGTACGCGGAATACTTCGA-3′. Knockdown efficiency was determined by western blotting.

2.8 | Generation of the rabbit anti-CD146 polyclonal antibody

Anti-peptide serum specific for the extracellular domain of CD146 was generated by injecting immunizing peptides into 2 rabbits (Sigma-Aldrich Japan), as previously described.[15] Specificity of the antibody was confirmed by immunofluorescence using IMR-32 and Mewo cell lines as positive and negative controls, respectively (Figure S1A, B).

2.9 | Measurement of cell viability, and performance of apoptosis and proliferation assays

Cell viability was measured using a WST-8 assay as described previously.[15] Apoptosis was examined by annexin V/7-amino-actinomycin D (AAD) co-staining (BD Biosciences), as described.[15] Annexin V^+ 7-AAD^- cells were considered as those in early apoptosis.

2.10 | Tumor implantation into NOG mice and serial transplantation

NB cell lines were treated with 0.05% trypsin/EDTA (Thermo Fisher Scientific) and the resultant single cells were resuspended in RPMI-1640 medium; 1.0×10^6 tumor cells were subcutaneously injected into the flanks of NOG mice using 27-gage needles. For fresh tumor samples, specimens obtained by surgery or biopsy procedures were cut up into evenly sized pieces (ie, 2 mm^3) with scissors. Each piece of primary tumor was then subcutaneously implanted into the flanks of NOG mice. Tumor formation was serially evaluated up to 60-100 d after implantation, when all mice were killed and subjected to the additional experiments. Serial transplantations were performed as described for fresh tumor samples.

2.11 | In vivo anti-tumor activity of shRNA-mediated knockdown of CD146 and of the anti-CD146 polyclonal antibody

At 1 wk after injection of 1.0×10^6 IMR-32 or RT-BM1 cells (n = 4 per condition), or soon after injection of 1.0×10^6 primary NB cells (n = 5 per condition), into the flank, NOG mice received anti-CD146 polyclonal antibody or rabbit normal IgG purified on a peptide column (800 μg/kg, twice a week until mice were euthanized). To silence CD146, 1.0×10^6 shRNA-treated NB cells were injected subcutaneously into the flanks of NOG mice (n = 4 per condition). After confirming tumor engraftment, doxycycline treatment was initiated. Measurement and histological analysis of engrafted tumors were performed as previously described.[15]

2.12 | Statistical analysis

The characteristics of the patients in the 2 groups were compared using Fisher exact test for categorical variables. Data are expressed as the mean ±SD. Differences in the mean values between groups were analyzed using Student *t* test and the Mann-Whitney

U test. Multiple comparisons were made using one-way or two-way ANOVA with the post-hoc Bonferroni multiple comparisons test. Estimates of variation within each group were made; variances were similar between statistically compared groups. The probability of OS and PFS rate was estimated using the Kaplan-Meier method, and a log-rank test was used for univariate analysis. For the animal studies, sample size was estimated as at least 4 mice per group to ensure sufficient power for statistical confidence. All statistical analyses were performed using EZR (version 1.32, Saitama Medical Center, Jichi Medical University), which is a graphical user interface for R (the R Foundation for Statistical Computing).[22] All *P*-values are two-sided. A *P*-value < .05 was considered significant for all analyses.

3 | RESULTS

3.1 | CD146 is expressed by most NB cells

First, we performed flow cytometry analysis to examine the expression of CD146 by NB cell lines and primary NB tumors. Table S2 demonstrates the cytogenic features of the 4 cell lines, which have been reported previously.[23-27] The median expression level of CD146 by all NB cell lines tested was 98.8% (range, 93.1-99.9; Figure 1A). The median expression level of CD146 by 15 NB primary tumors was 93.5% (range, 12.2-99.3; Figure 1B, C).

Next, we performed immunohistochemical analysis to examine expression of CD146 by NB primary tumors. Patient and tumor characteristics of the 41 patients were presented in Table S3. Typically, expression was detected in undifferentiated neuroblasts (Figure 1D), mature Schwann cells, and ganglion cells. The median H-score of CD146 immunostaining in the 41 NB primary tumors was 199 (range, 2-289). There were no significant differences in 3-y OS (84.2%; 95% confidence interval [CI], 58.7%-94.6% vs. 82.5%; 95% CI, 54.9%-94.0%; *P* =.918; Figure 1E) and PFS rates (64.5%; 95% CI, 39.5%-81.4% vs. 72.2%; 95% CI, 45.4%-87.4%; *P* =.338; Figure 1F) between the CD146^{low} (H-score <200) and CD146^{high} (H-score ≥200) groups. As expected, univariate analysis identified age, stage, histology, and MYCN amplification as risk factors for OS and/or PFS (Table S4). Patients in the CD146^{high} groups were more likely to have stages 2 and 3 disease, and there was no other significant difference between these prognostic factors and CD146 positivity (Table S5). As the gene encoding *CD146* is located in 11q23.3, which is frequently deleted in stage 4 neuroblastomas,[28] we next analyzed the relationship between *CD146* expression and 11q copy-number status using publicly available whole exome and transcriptome sequencing data of 105 high-risk neuroblastomas generated by the TARGET initiative (http://ocg.cancer.gov/programs/target). Among

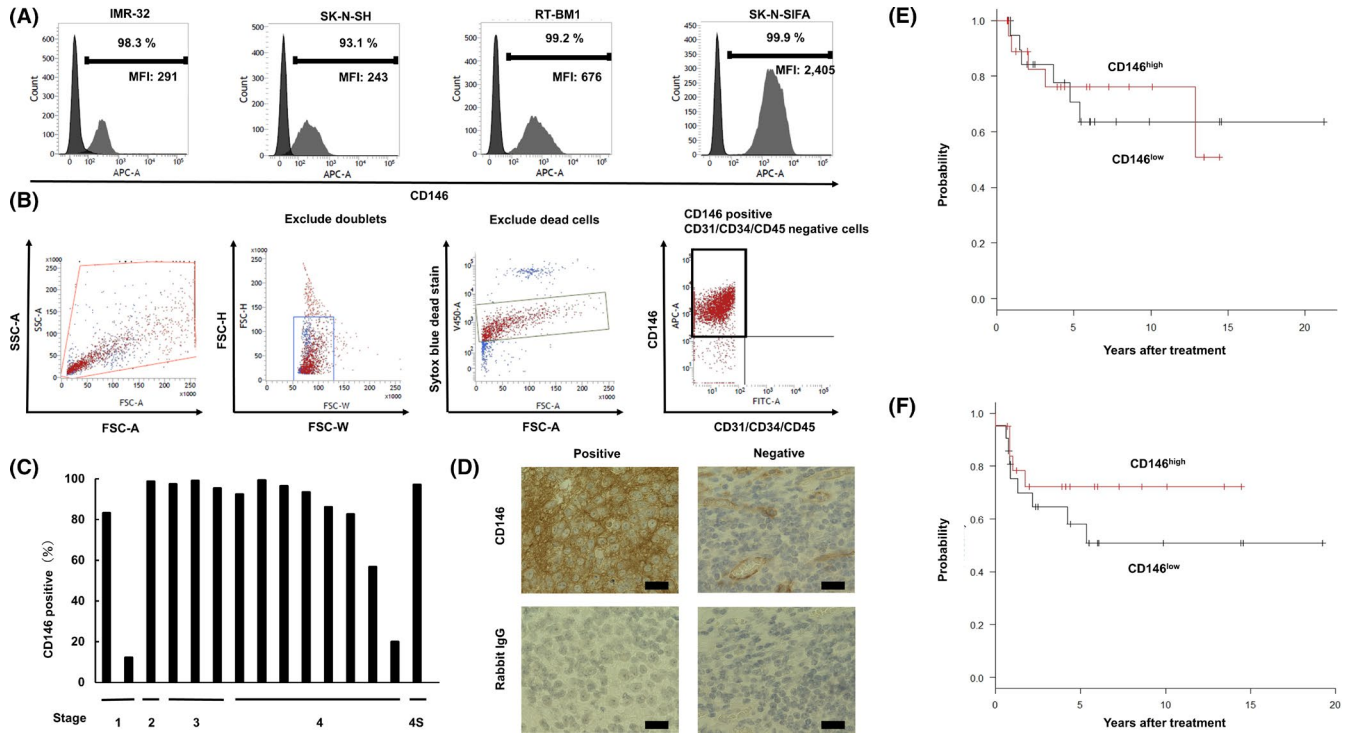

FIGURE 1 Flow-cytometric analysis of CD146 expression by NB cell lines and primary tumors. A, Representative plots showing NB primary tumors stained with the anti-CD146 antibody (gray histogram) or an isotype-matched control antibody (black histogram). MFI, mean fluorescence intensity. B, Gating strategy for flow-cytometric analysis of primary NB tumors, showing that a small CD146-expressing subpopulation (boxed region) was present in the rightmost plot. C, Expression of CD146 by NB primary tumors. D, Immunohistochemical images of NB primary tumors stained with the anti-CD146 antibody. Scale bars, 20 μm. E, F, Overall survival (E) and PFS rates (F) of the CD146^{high} and CD146^{low} groups

these 105 neuroblastomas, 59 harbored an 11q deletion and showed significantly lower *CD146* expression levels compared with those without the deletion (P =.016; Figure S2). Nonetheless, CD146 was expressed broadly by NB primary tumors of any stage and with different prognoses.

3.2 | CD146 efficiently suppresses survival of NB cells by inducing apoptosis

To investigate the anti-tumor effects of blocking CD146-related signals in NB cells, we constructed a tetracycline-inducible shRNA-mediated CD146-knockdown system, as previously reported.[21] The transfection efficiency of CD146-shRNA1, CD146-shRNA2, and luciferase (Luc)-shRNA was confirmed by western blotting (Figure 2A). WST-8 and sphere-forming assays demonstrated that knockdown of *CD146* significantly reduced survival and anchorage-independent growth, respectively, of NB cells (Figure 2B, C). Furthermore, apoptosis assays revealed that knocking down *CD146* led to a significant increase in the number of annexin V^+ 7-AAD^- early apoptotic cells (Figure 2D, E).

To identify signaling transduction pathways involved in CD146-associated apoptosis in NB cells, we examined the activity of FAK, nuclear factor-kappa B (NF-κB), Akt, and p38 MAPK, all of which are downstream targets of CD146.[10] Conditional knockdown of *CD146* reduced phosphorylation of FAK and NF-κB, but not that of Akt or p38 MAPK (Figure 2F, G and Figure S3A,B). Therefore, blocking CD146 increased apoptosis of NB cells via the FAK and/or NF-κB signaling pathway.

Next, we investigated the in vivo anti-tumor effects of sustained conditional knockdown of CD146 in a xenograft model based on immunodeficient NOG mice. Both tumor volume and weight fell markedly by sustained shRNA-mediated CD146 knockdown; these in vivo anti-tumor effects were sustained for up to 14 d post-transplantation (Figure 3A-C). Histological analysis of tumors in NOG mice revealed clusters of small round GD2-positive tumor cells without identifiable neuropils (Figure S4A), similar to the histological findings in NB tumors. Furthermore, immunostaining for single-stranded DNA revealed that conditional knockdown of *CD146* increased the number of apoptotic cells (Figure 3D). CD146 was faintly expressed in engrafted tumors following continuous tetracycline treatment (Figures 3E and S4B), confirming sustained, although not complete, knockdown of CD146 expression. No distant metastasis, including bone marrow metastasis, was visible macroscopically in either CD146 or Luc knockdown mice. Therefore, blocking CD146-related mechanisms efficiently suppressed growth of NB tumors in vivo by inducing apoptosis.

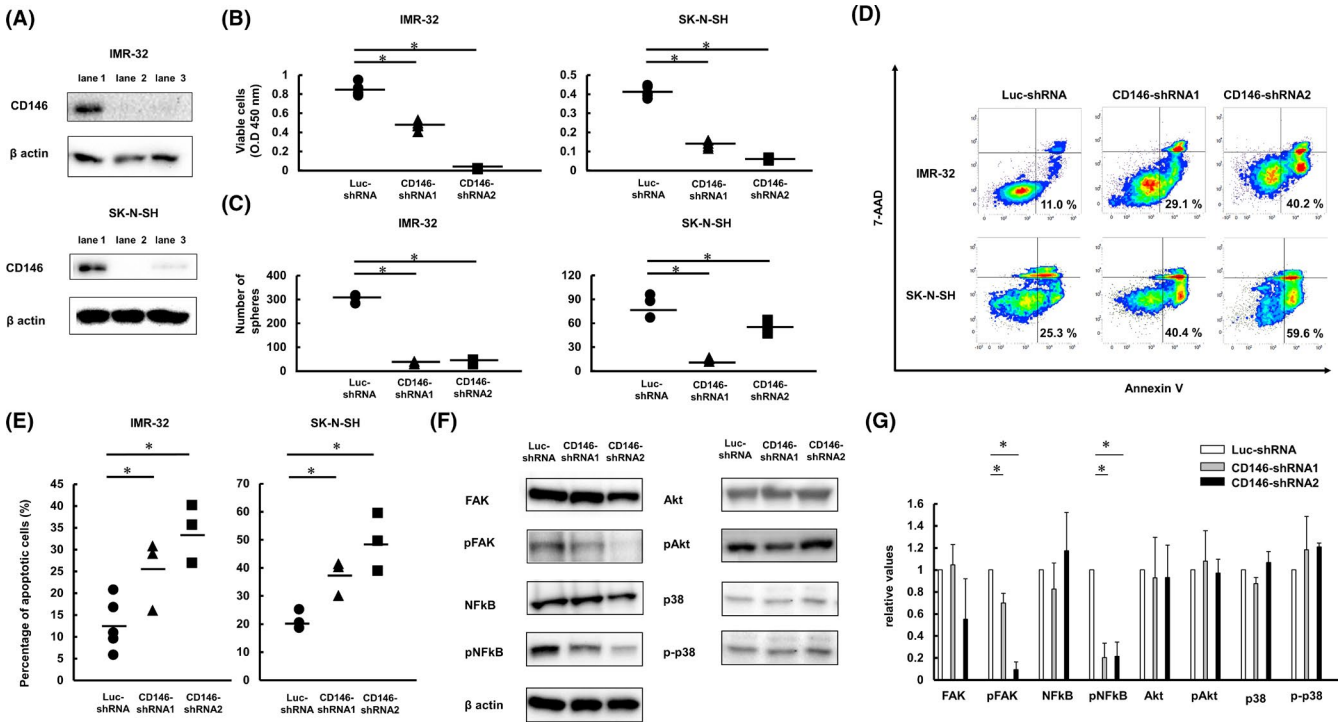

FIGURE 2 In vitro anti-tumor effects of CD146 knockdown in IMR-32 and SK-N-SH NB cells. A, Western blotting to detect expression of CD146 and β-actin after shRNA transduction (lane 1, Luc-shRNA; lane 2, CD146-shRNA1; lane 3, CD146-shRNA2). B, WST-8 assays after shRNA transduction. Data are presented as the actual absorbance values after shRNA transduction. C, Sphere-forming assays after shRNA transduction. D, Representative flow-cytometric profiles showing apoptosis. E, Apoptosis assay after shRNA transduction. F, G, Representative western blot images (F) and densitometric analysis for the expression of FAK, phosphorylated FAK, NF-κB, phosphorylated NF-κB, Akt, phosphorylated Akt; p38 MAPK, phosphorylated p38 MAPK; and β-actin (G) after shRNA transduction. Error bars indicate the SD. Results are representative of 3 independent experiments (*P < .05)

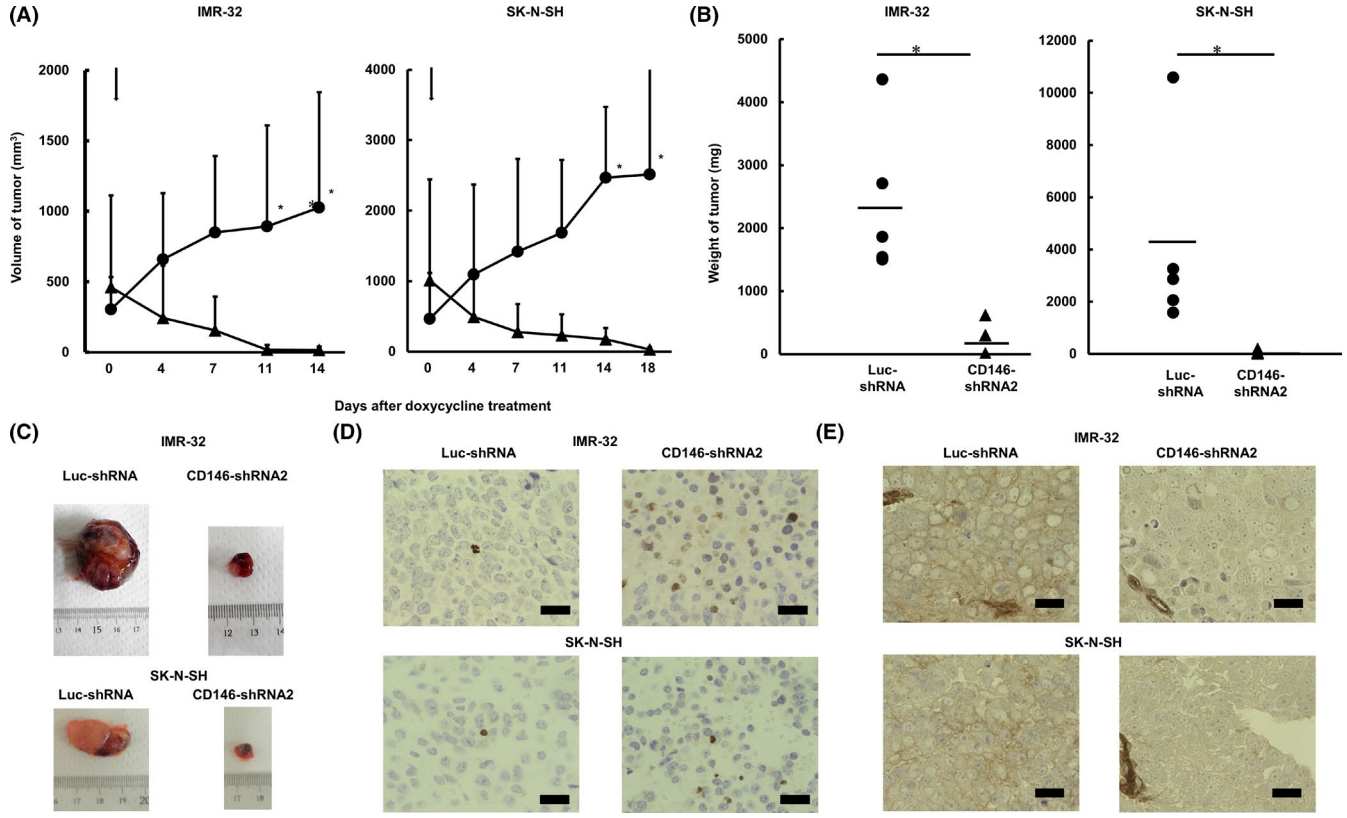

FIGURE 3 In vivo anti-tumor effects of CD146 knockdown in IMR-32 and SK-N-SH NB cells. A, Volume of tumor cell xenografts in NOG mice after transduction of CD146-shRNA (triangles) and Luc-shRNA (circles). Arrows indicate the day of doxycycline treatment. B, Effect on tumor weight. C, Macroscopic appearance of tumor tissues. D, E, Immunohistochemical images of tumor tissues stained with anti-single-stranded DNA (D) and anti-CD146 antibodies (E). Scale bars, 20 μm

3.3 | Targeting CD146 inhibits in vitro proliferation of NB cells and in vivo growth of NB tumors

To examine novel immunotherapies for NB, we next investigated the anti-tumor effects of a recently developed rabbit anti-CD146 polyclonal antibody.[15] Exposure of NB cells to the anti-CD146 antibody led to a significant reduction in survival and anchorage-independent growth (Figures 4A, B, and S5A). Non-specific cytotoxic effects were excluded because the antibody did not have adverse effects on a Mewo melanoma cell line, which barely expresses CD146 (Figure S5B, C).

Next, we investigated the anti-tumor effects of the rabbit anti-CD146 polyclonal antibody. Within 3 to 4 wk after treatment, massive subcutaneous tumors were found in mice treated with normal rabbit IgG. By contrast, intraperitoneal injection of the anti-CD146 antibody into NOG mice for ~50 d led to a significant inhibition of tumor growth (Figure 4C-E). Furthermore, immunostaining for single-stranded DNA revealed that apoptotic cells were more abundant in mice treated with purified anti-CD146 antibody compared with mice treated with normal rabbit IgG (Figure 4F). The expression level of CD146 in engrafted tumors following the anti-CD146 antibody was almost negligible (Figure 4G). Previous reports have shown that the anti-CD146 antibody exhibits anti-tumor effects against various malignancies by inhibiting intratumoral angiogenesis.[13,29,30] Here, we found that the anti-CD146 antibody also inhibited survival of HUVECs, which express CD146 at high levels (Figure S5D). However, immunohistochemical analysis of CD31 expression revealed no significant difference in microvessel density between mice treated with the anti-CD146 antibody and mice treated with normal rabbit IgG (Figure S5E), suggesting that the inhibitory effect of the anti-CD146 antibody on tumor neovascularization was almost negligible.

Finally, we used a xenograft model based on patient-derived tumor cells to assess the utility of the anti-CD146 antibody for treatment of primary NB tumors. Successful serial engraftment of $CD146^+$ cells was observed after subcutaneous injection of early passage NB primary cell xenografts. The engrafted tumors were predominantly $CD146^+$ cells after serial transplantation (Figure 5A). Invasion of NB tumor cells was confirmed histologically by H&E staining and by immunostaining for GD2 (Figure 5B). Tumor volume in mice treated with the anti-CD146 antibody was significantly lower compared with that in mice treated with normal rabbit IgG (P =.036; Figure 5C, D). There was also a difference in tumor weight, although this was of borderline significance (P =.093; Figure 5E). Furthermore, anti-CD146 antibody led to a marked increase in the number of

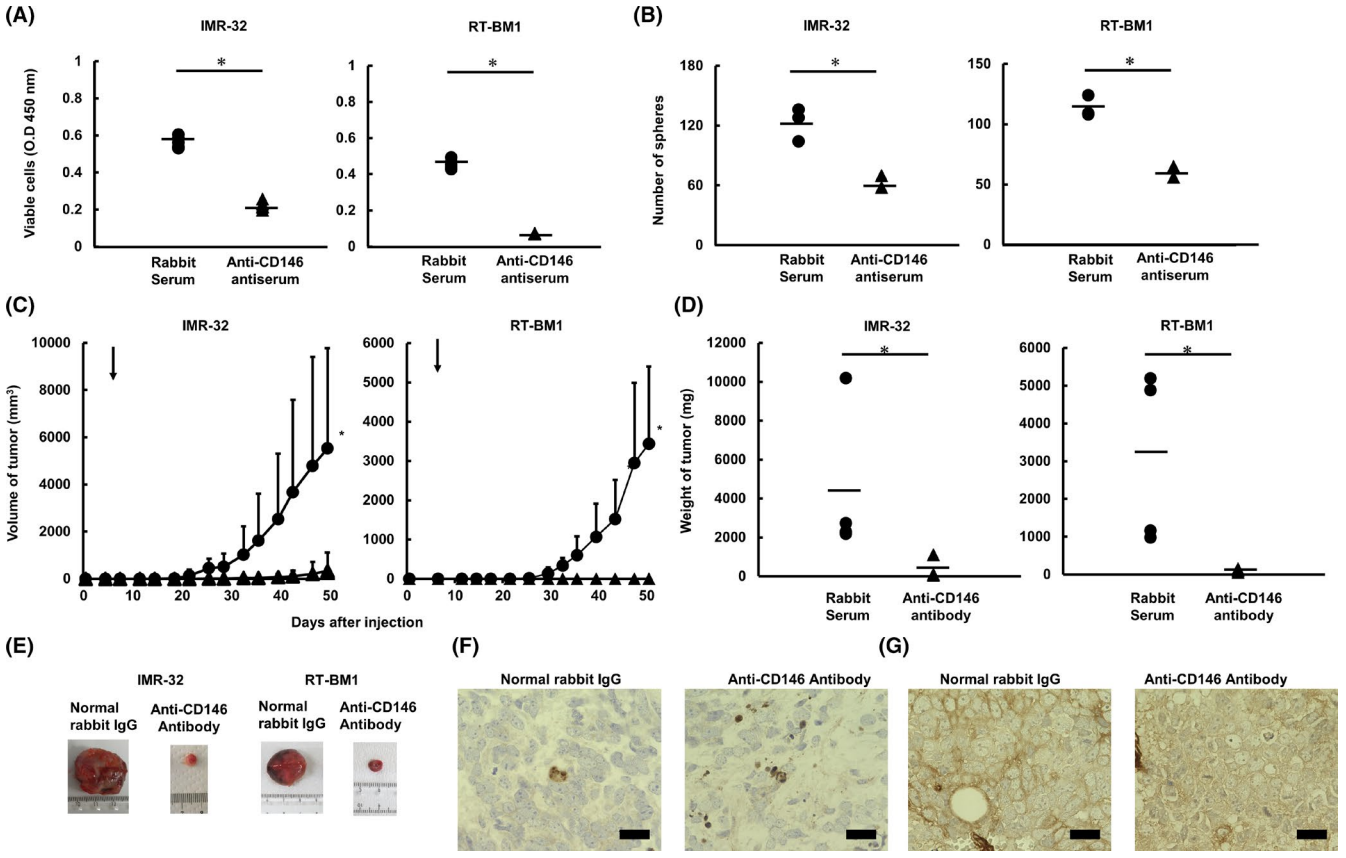

FIGURE 4 Anti-tumor activity of the anti-CD146 polyclonal antibody against IMR-32 and RT-BM1 NB cells. A, B, WST (A) and sphere-forming assay (B) after treatment with normal rabbit serum or anti-CD146 antiserum. OD, optical density. Data are presented as the actual absorbance values after treatment in (A). C, In vivo anti-tumor effect of the purified anti-CD146 antibody (triangles) and normal rabbit IgG (circles) on the volume of tumor cell xenografts in NOG mice. Arrows indicate the day of treatment. D, Effect on tumor weight. E, Macroscopic appearance of tumor tissues. F, G, Immunohistochemical images showing tumor tissues stained with anti-single-stranded DNA (F) and anti-CD146 antibodies (G). Scale bars, 20 μm. Error bars indicate the SD. Results are representative of 3 independent experiments (*$P < .05$)

single-stranded DNA-positive apoptotic cells (Figure 5F). The expression level of CD146 in engrafted tumors following anti-CD146 antibody treatment was almost negligible (Figure 5G).

4 | DISCUSSION

Here, we provide evidence that blocking CD146-related mechanisms, either by treatment with an anti-CD146 polyclonal antibody or by shRNA-mediated knockdown of CD146, effectively suppresses the growth of NB cells both in vitro and in vivo. Of note, a high percentage of CD146-expressing cells were present within tumor samples from most NB patients with various clinicopathological and genetic prognostic factors. However, the analysis of deposit whole exome and transcriptome sequencing data demonstrated that the expression level of CD146 was significantly lower in a subgroup with the 11q deletion with poor prognosis.[28] Therefore, further studies using patient-derived tumor cells will be required to investigate the efficacy of CD146-targeted therapy for this group.

NK–cell-mediated ADCC is mandatory for the efficacy of anti-GD2 antibody therapy.[31] However, antibody-mediated anti-tumor effects are attenuated in a subgroup of patients expressing specific inhibitory killer immunoglobulin-like receptors and human leukocyte antigen class I ligands.[32] Here, we used heat-inactivated serum (ie, in the absence of complement) to show that the anti-CD146 antibody exhibited anti-tumor effects in vitro, and tumor-bearing NOG mice lacking functional macrophages and NK cells to show anti-tumor effects in vivo. Therefore, the antibody does not function by triggering complement-dependent cytotoxicity or ADCC; rather, it triggers apoptosis directly, as reported for malignant rhabdoid tumor.[15] The potential immune system-independent mechanisms associated with the anti-tumor effects of anti-CD146 antibody, including inhibition of adhesion and/or ligand binding and induction of growth suppressive signaling, are of great biological interest. We speculate that all patients with NB that expresses CD146 will benefit from treatment with this antibody, irrespective of anti-tumor immune response status. Furthermore, immunocombination therapy, such as anti-GD2 antibody treatment followed by anti-CD146 antibody treatment,

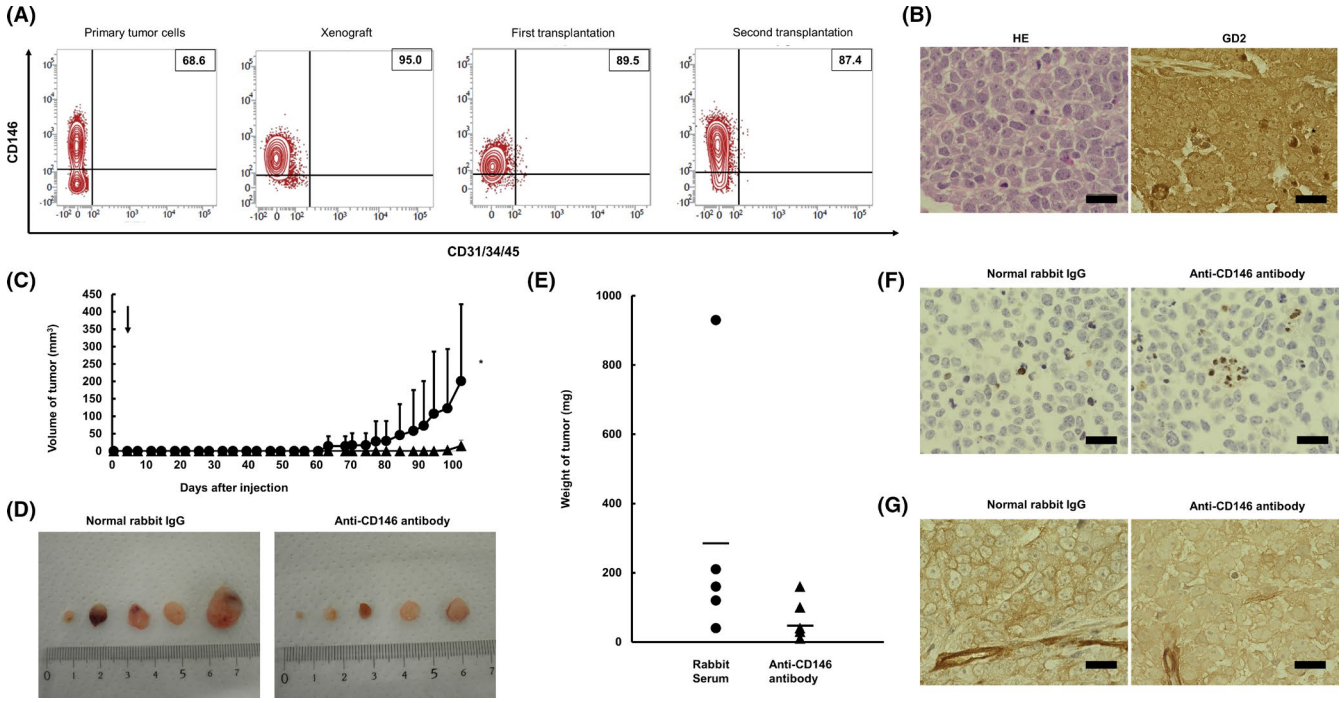

FIGURE 5 Anti-tumor activity of the anti-CD146 polyclonal antibody against NB primary tumors. A, Serial flow-cytometric analysis of CD146 expression by engrafted NB primary tumor cells during serial transplantation. B, H&E and immunostaining for GD2 in a tumor generated from an early passage xenograft from a NB primary tumor. C, Anti-tumor effect of the purified anti-CD146 antibody (triangles) or normal rabbit IgG (circles) on the volume of tumor cell xenograft tumors in NOG mice (*$P < .05$). D, Macroscopic appearance of tumor tissues. E, Effect on tumor weight. F, G, Immunohistochemical images of tumor tissues stained with anti-single-stranded DNA (F) and anti-CD146 antibodies (G). Scale bars, 20 μm

would exert synergistic efficacy for patients with NB with the potential to mount an immune response.

Blocking CD146-related signals induced apoptosis in all 4 NB cell lines via the FAK and/or NF-κB signaling pathways. NF-κB inhibition sensitizes NB cells to Fas- or TRAIL-induced apoptosis[33,34]: Furthermore, anti-CD146 monoclonal antibody exerts an inhibitory effect of angiogenesis by suppressing NF-κB activity.[35] FAK is a cytoplasmic tyrosine kinase that plays roles in a wide range of fundamental cellular processes, including cell survival, proliferation, adhesion, and apoptosis, through integrin- or surface receptor-mediated signaling pathways.[36] FAK is overexpressed in various types of cancer, including NB,[36-38] and is associated with CD146.[39,40] FAK is closely related to loss of adhesion and induction of apoptosis; this process, called anoikis, is triggered when anchorage-dependent cells lose attachment to the surrounding extracellular matrix.[41,42] However, sphere-forming assays revealed that silencing of CD146 led to a significant reduction in anchorage-independent growth of NB cells, suggesting involvement of alternative CD146-mediated, FAK-independent signaling pathways.

There have been several reports on the association of CD146 promotes with metastasis in various malignancies.[11,13] In this study, we failed to address whether blocking CD146-related signals inhibited the metastatic ability of NB, as no distant metastasis was observed after subcutaneous implantation of NB cells in NOG mice. Orthotopic inoculation of NB cells, which enables a higher degree of distant metastasis,[43] might aid further investigation for the inhibitory effect of CD146 blocking on NB metastasis.

Targeting activated signaling transduction pathways in selected malignancies, using antibodies or small molecular inhibitors, is of great utility as a potential anticancer therapy; however, there are serious concerns about potential toxicity, especially in infants and children. CD146 is expressed widely in the nervous system and is involved in several neural processes.[44,45] Furthermore, nervous system-specific knockout of CD146 in mice resulted in decreased appetite and locomotor activity, along with impaired spatial learning and memory.[46] CD146 is also abundantly expressed in endothelial cells and pericytes, and has an important role in vessel permeability and angiogenesis.[47] Therefore, penetration of the blood-brain barrier and bleeding risk by the antibody should be assessed before clinical use. Alternatively, antibody against the soluble form of CD146 might avoid such toxicities.[48]

Immunotherapy with monoclonal antibodies is used widely in patients with hematological malignancies and in adults with solid tumors.[49] However, such therapeutic approaches have not been realized fully in pediatric solid tumors. Previously, we showed that CD146 is expressed by other types of pediatric solid tumors, including Ewing sarcoma, malignant glioma, and hepatoblastoma (Obu S, Sonoda M, Umeda K, et al, unpublished data). The findings of this study might extend the application of CD146-targeting therapy for a broad range of CD146-expressing pediatric tumors.

ACKNOWLEDGMENTS

We thank all staff for help with histological analysis. The current study was supported by grants from the Grant-in-Aid for Scientific Research (C) (15K09651) and (B) (21H02880), the Project for Cancer Research and Therapeutic Evolution (16cm0106509h001), and the Practical Research for Innovative Cancer Control (19ck0106468h0001) by Japan Agency for Medical Research and Development, the Project Mirai Cancer Research Grants, and Bristol-Myers Squibb.

DISCLOSURE

The authors have no conflicts of interest to declare.

ORCID

Katsutsugu Umeda https://orcid.org/0000-0002-6844-2011
Hiroo Ueno https://orcid.org/0000-0001-7617-1672
Keiji Tasaka https://orcid.org/0000-0002-2708-3876
Satoshi Saida https://orcid.org/0000-0002-8930-3539
Itaru Kato https://orcid.org/0000-0002-2932-4960
Hidefumi Hiramatsu https://orcid.org/0000-0003-3136-5670
Tatsuya Okamoto https://orcid.org/0000-0003-1958-0714
Eri Ogawa https://orcid.org/0000-0003-3642-8802
Hideaki Okajima https://orcid.org/0000-0002-4043-1070
Ken Morita https://orcid.org/0000-0002-6639-5274
Yasuhiko Kamikubo https://orcid.org/0000-0003-2761-8508
Koji Kawaguchi https://orcid.org/0000-0002-4612-4047
Kenichiro Watanabe https://orcid.org/0000-0002-8892-3082
Hideto Iwafuchi https://orcid.org/0000-0002-7755-9676
Shigeki Yagyu https://orcid.org/0000-0003-4256-9783
Tomoko Iehara https://orcid.org/0000-0003-1740-7096
Hajime Hosoi https://orcid.org/0000-0002-8345-0159
Tatsutoshi Nakahata https://orcid.org/0000-0003-0427-8440
Souichi Adachi https://orcid.org/0000-0002-8473-0187
Shinji Uemoto https://orcid.org/0000-0003-0126-9346
Toshio Heike https://orcid.org/0000-0002-6373-3442
Junko Takita https://orcid.org/0000-0002-2452-6520

REFERENCES

1. Smith MA, Altekruse SF, Adamson PC, et al. Declining childhood and adolescent cancer mortality. *Cancer*. 2014;120:2497-2506.
2. Pinto NR, Applebaum MA, Volchenboum SL, et al. Advances in risk classification and treatment strategies for neuroblastoma. *J Clin Oncol*. 2015;33:3008-3017.
3. London WB, Castel V, et al. Clinical and biologic features predictive of survival after relapse of neuroblastoma: a report from the International Neuroblastoma Risk Group project. *J Clin Oncol*. 2011;29:3286-3292.
4. Perwein T, Lackner H, Sovinz P, et al. Survival and late effects in children with stage 4 neuroblastoma. *Pediatr Blood Cancer*. 2011;57:629-635.
5. Yu AL, Gliman AL, Pzkaynak MF, et al. Anti-GD2 antibody with GM-CSF, interleukin-2, and isotreinoin for neuroblastoma. *N Engl J Med*. 2010;363:1324-1334.
6. Shusterman S, London WB, Gillies SD, et al. Antitumor activity of hu14.18-IL2 in patients with relapsed/refractory neuroblastoma: A Children's Oncology Group (COG) phase II study. *J Clin Oncol*. 2010;28:4969-4975.
7. Crane JF, Trainor PA. Neural crest stem and progenitor cells. *Ann Rev Cell Dev Biol*. 2006;22:267-286.
8. Kuske MD, Johnson JP. Assignment of the human melanoma cell adhesion molecule gene (MCAM) to chromosome 11 band q23.3 by radiation hybrid mapping. *Cytogenet Cell Genet*. 1999;87:258.
9. Shih IM, Nesbit M, Herlyn M, et al. A new Mel-CAM (CD146) specific monoclonal antibody, MN-4, on paraffin embedded tissue. *Mod Pathol*. 1998;11:1098-1106.
10. Shih IM. The role of CD146 (Mel-CAM) in biology and pathology. *J Pathol*. 1999;189:4-11.
11. Wang Z, Yan X. CD146, a multi-functional molecule beyond adhesion. *Cancer Lett*. 2013;330:150-162.
12. Pujages C, Guez-Guez B, Dunon D. Melanoma cell adhesion molecule (MACM) expression in the myogenic lineage during early chick embryonic development. *Int J Dev Biol*. 2002;46:263-266.
13. Mills L, Tellez C, Huang S, et al. Fully human antibodies to MCAM/MUC18 inhibit tumor growth and metastasis of human melanoma. *Cancer Res*. 2002;62:5106-5104.
14. Maguire LH, Thomas AR, Goldstein AM. Tumors of the neural crest: Common themes in development and cancer. *Dev Dyn*. 2015;244:311-322.
15. Nodomi S, Umeda K, Saida S, et al. CD146 is a novel marker for highly tumorigenic cell and a potential therapeutic target in malignant rhabdoid tumor. *Oncogene*. 2016;35:5317-5327.
16. Orentas RJ, Yang JJ, Wen X, et al. Identification of cell surface proteins as potential immunotherapy targets in 12 pediatric cancers. *Front Oncol*. 2012;2:194.
17. Sugimoto T, Gotoh T, Yagyu S, et al. A MYCN-amplified cell line derived from a long-term event-free survivor among our sixteen established neuroblastoma cell lines. *Cancer Lett*. 2013;331:115-121.
18. Shimada H, Ambros IM, Dehner LP, et al. The international neuroblastoma pathology classification (the Shimada system). *Cancer*. 1999;86:364-372.
19. Brodeur GM, Pritchard J, Berthold F, et al. Revisions of the international criteria for neuroblastoma diagnosis, staging, and response to treatment. *J Clin Oncol*. 1993;11:1466-1477.
20. Avilés-Salas A, Muñiz-Hernández S, Maldonado-Martínez HA, et al. Reproducibility of the EGFR immunohistochemistry scores for tumor samples from patients with advanced non-small cell lung cancer. *Oncol Lett*. 2017;13:912-920.
21. Morita K, Suzuki K, Maeda S, et al. Genetic regulation of the RUNX transcription factor family has antitumor effects. *J Clin Invest*. 2017;127:2815-2828.
22. Kanda Y. Investigation of the freely available easy-to-use software 'EZR' for medical statistics. *Bone Marrow Transplant*. 2013;48:452-458.
23. Bogen D, Wei JS, Azorsa DO, et al. Aurora B kinase is a potent and selective target in MYCN-driven neuroblastoma. *Oncotarget*. 2015;6:35247-35262.
24. Erdreich-Epstein A, Singh AR, Joshi S, et al. Association of high microvessel αvβ3 and low PTEN with poor outcome in stage 3 neuroblastoma: rationale for using first in class dual PI3K/BRD4 inhibitor, SF1126. *Oncotarget*. 2016;8:52193-52210.
25. Gu L, Chu P, Lingeman R, et al. The mechanism by which MYCN amplification confers an enhanced sensitivity to a PCNA-derived cell permeable peptide in neuroblastoma cells. *EBioMedicine*. 2015;2:1923-1931.
26. Terui E, Matsunaga T, Yoshida H, et al. Shc family expression in neuroblastoma: high expression of shcC is associated with a poor prognosis in advanced neuroblastoma. *Clin Cancer Res*. 2005;11:3280-3287.
27. Sugino Y, Misawa A, Inoue J, et al. Epigenetic silencing of prostaglandin E receptor 2 (PTGER2) is associated with progression of neuroblastomas. *Oncogene*. 2007;26:7401-7413.

28. Guo C, White PS, Weiss MJ, et al. Allelic deletion at 11q23 is common in MYCN single copy neuroblastoma. *Oncogene*. 1999;18:4948-4957.
29. Yan X, Lin Y, Yang D, et al. A novel anti-CD146 monoclonal antibody, AA98, inhibits angiogenesis and tumor growth. *Blood*. 2003;102:184-191.
30. McGary EC, Heimberger A, Mills L, et al. A fully human antimelanoma cellular adhesion molecule/MUC18 antibody inhibits spontaneous pulmonary metastasis of osteosarcoma cells in vivo. *Clin Cancer Res*. 2013;9:6560-6566.
31. Barker E, Mueller BM, Handgretinger R, et al. Effect of a chimeric anti-ganglioside GD2 antibody on cell-mediated lysis of human neuroblastoma cells. *Cancer Res*. 1991;51:144-149.
32. Forlenza CJ, Boudreau JE, Zheng J, et al. KIR3DLI allelic polymorphism and HLA-B epitopes modulate response to anti-GD2 monoclonal antibody in patients with neuroblastoma. *J Clin Oncol*. 2016;34:2443-2451.
33. Ammann JU, Haag C, Kasperczyk H, et al. Sensitization of neuroblastoma cells for TRAIL-induced apoptosis by NF-kappaB inhibition. *Int J Cancer*. 2009;124:1301-1311.
34. Yang HJ, Wang M, Wang L, et al. NF-κB regulates caspase-4 expression and sensitizes neuroblastoma cells to Fas-induced apoptosis. *PLoS One*. 2015;19:e0117953.
35. Bu P, Gao L, Zhuang J, et al. Anti-CD146 monoclonal antibody AA98 inhibits angiogenesis via suppression of nuclear factor-KB activation. *Mol Cancer Ther*. 2006;5:2872-2878.
36. Zhou J, Yi Q, Tang L. The roles of nuclear focal adhesion kinase (FAK) on cancer: a focused review. *J Exp Clin Cancer Res*. 2019;38:250.
37. Beierle EA, Trujillo A, Nagaram A, et al. N-MYC regulates focal adhesion kinase expression in human neuroblastoma. *J Biol Chem*. 2007;282:12503-12516.
38. Beierle EA, Massoll NA, Hartwich J, et al. Focal adhesion kinase expression in human neuroblastoma: immunohistochemical and real-time PCR analyses. *Clin Cancer Res*. 2008;14:3299-3305.
39. Anfosso F, Badtin N, Francès V, et al. Activation of human endothelial cells via S-endo-1 antigen (CD146) stimulates the tyrosine phosphorylation of focal adhesion kinase p125 (FAK). *J Biol Chem*. 1998;273:26852-26856.
40. Jouve N, Bachelier R, Despoix N, et al. CD146 mediates VEGF-induced melanoma cell extravasation through FAK activation. *Int J Cancer*. 2015;137:50-60.
41. Frisch SM, Vuori K, Ruhoslahti E, et al. Control of adhesion-dependent cell survival by focal adhesion kinase. *J Cell Biol*. 1996;134:793-799.
42. Paoli P, Giannoni E, Chiarugi P. Anoikis molecular pathway and its role in cancer progression. *Biochem Biophys Acta*. 2013;1833:3481-3498.
43. Braekeveldt N, Wigerup C, Gisselsson D, et al. Neuroblastoma patient-derived orthotopic xenografts retain metastatic patterns and geno- and phenotypes of patient tumours. *Int J Cancer*. 2015;136:E252-261.
44. Schwarz MJ, Müller N, Körschenhausen D, et al. Melanoma-associated adhesion molecule MUC/MCAM (CD146) and transcriptional regulator mader in normal human CNS. *NeuroImmunoModulation*. 1998;5:270-276.
45. Taira E, Kohama K, Tsukamoto Y, et al. Characterization of Gicerin/MUC18/CD146 in the rat nervous system. *J Cell Physiol*. 2004;198:377-387.
46. Tu T, Gao Q, Luo Y, et al. CD146 depletion in the nervous system impairs appetite, locomotor activity and spatial learning in mice. *PLoS One*. 2013;8:e74124.
47. Leroyer AS, Blin MG, Bachelier R, et al. CD146 (Cluster of differentiation 146). *Arterioscler Thromb Vasc Biol*. 2019;39:1026-1033.
48. Stalin J, Trabousi W, Vivancos-Stalin L, et al. Therapeutic targeting of soluble CD146/MCAM with the M2J–1 monoclonal antibody prevents metastasis development and procoagulant activity in CD146-positive invasive tumors. *Int J Cancer*. 2020;147:1666-1679.
49. Palanca-Wessels MC, Press OW. Advances in the treatment of hematologic malignancies using immunoconjugates. *Blood*. 2014;123:2293-2301.

SUPPORTING INFORMATION

Additional supporting information may be found online in the Supporting Information section.

How to cite this article: Obu S, Umeda K, Ueno H, et al. CD146 is a potential immunotarget for neuroblastoma. *Cancer Sci*. 2021;112:4617–4626. https://doi.org/10.1111/cas.15124